**Computers and Concrete**, *Vol. 14, No. 5 (2014) 527-546*
DOI: http://dx.doi.org/10.12989/cac.2014.14.5.527 

# Study on fracture behavior of polypropylene fiber reinforced concrete with bending beam test and digital speckle method

Peng Cao[1a], Decheng Feng[2b], Changjun Zhou[*2] and Wenxin Zuo[3c]

[1]*Department of Hydraulic Engineering, Tsinghua University, Beijing, 100084, China*
[2]*School of Transportation Science and Engineering, Harbin Institute of Technology, 73 Huagnhe Street, Harbin, 150090, China*
[3]*School of Civil Engineering, University of Birmingham, UK, B15 2TT*

(*Received January 25, 2014, Revised July 10, 2014, Accepted July 25, 2014*)

**Abstract.** Portland cement concrete, which has higher strength and stiffness than asphalt concrete, has been widely applied on pavements. However, the brittle fracture characteristic of cement concrete restricts its application in highway pavement construction. Since the polypropylene fiber can improve the fracture toughness of cement concrete, Polypropylene Fiber-Reinforced Concrete (PFRC) is attracting more and more attention in civil engineering. In order to study the effect of polypropylene fiber on the generation and evolution process of the local deformation band in concrete, a series of three-point bending tests were performed using the new technology of the digital speckle correlation method for FRC notched beams with different volumetric contents of polypropylene fiber. The modified Double-K model was utilized for the first time to calculate the stress intensity factors of instability and crack initiation of fiber-reinforced concrete beams. The results indicate that the polypropylene fiber can enhance the fracture toughness. Based on the modified Double-K fracture theory, the maximum fracture energy of concrete with 3.2% fiber (in volume) is 47 times higher than the plain concrete. No effort of fiber content on the strength of the concrete was found. Meanwhile to balance the strength and resistant fracture toughness, concrete with 1.6% fiber is recommended to be applied in pavement construction.

**Keywords:** concrete; polypropylene fiber; three-point bending beam; pressure-cracking mouth opening displacement (P-CMOD); fracture

## 1. Introduction

### *1.1 Research background*

Portland cement concrete, which has higher strength and stiffness than asphalt pavement, has been widely applied on pavements. However, the brittle fracture characteristic of cement concrete restricts its use in the high grade pavement construction. Since the polypropylene fiber can

∗Corresponding author, Ph.D., Assistant Professor, E-mail: 4002cj@163.com
[a]Ph.D., Postdoctoral Research Associate, E-mail: caopeng518888@126.com
[b]Ph.D., Professor, E-mail: fengdecheng@hit.edu.cn
[c]Ph.D. student, E-mail: wenxinzuo@hotmail.com


 ISSN: 1598-8198 (Print), 1598-818X (Online)

improve the fracture toughness property of cement concrete pavement, Polypropylene Fiber-Reinforced Concrete (PFRC) is drawing more and more attention in pavement construction. Lots of researches have been conducted on the mechanical properties and durability of polypropylene fiber-reinforced concrete (Banthia and Nandakumar 2003; Katz and Bentur 1994; Tavakoli 1994; Toutanji 1999). Ramli *et al*. (2013) studied the durability of fiber-reinforced concrete in harsh environments. However, most studies were still focused on its basic performances, including the compressive strength, bending strength, frost resistance and impact resistance. There was few study involved in the fracture resistance of concrete, especially with varied volumetric contents of fiber. Usually, laboratory experiments were conducted to determine a proper content of fiber in the reinforced concrete, which is time-consuming and energy-exhausting. It would be beneficial for the fiber reinforce concrete structure construction if a theory can be utilized to quantitatively evaluate the fracture resistance of FRC and to guide the addition of fiber in cement concrete.

Fracture mechanics is a powerful tool for modeling the nonlinear fracture behavior of quasi-brittle materials subjected to a limited load. The solid fracture mechanics was first introduced by Griffith in the glass fracture. With the development of computational solid mechanics, the solid fracture mechanics has been more and more important in the evaluation of structure safety. Dugdale (1960) extended the application of fracture mechanics in the metal materials. Kaplan (1961) first introduced fracture mechanics to analyze the fracture of concrete. However, some researchers disagreed with the perspective that linear fracture mechanics could simulate the fracture behavior of cement concrete (Kesler and Naus 1972) and proposed many nonlinear fracture mechanics models. Based on the finite element method (FEM), Ngo and Scordelis (1967) introduced the separation cracking model to simulate the fracture behavior of the cement concrete. They suggested that the element nodal would be separated when the nodal force exceed the maximal strength. Rashid(1968) considered that the nodal separation should be led by the maximum principal stress, and such rotation cracking behavior could be explained by the separation cracking model. The most famous fracture model was proposed by Hillerberg *et al*. (1976), called Fictitious Crack Model (FCM). This model could simulate the softening behavior during the cracking evolution, and was widely utilized to investigate the fracture behaviors of concrete and rock. Oh and Bazant (1983) developed a new finite element fracture model called Blunt Crack Band Model, which could attenuate the sensitivity of mesh partition in FE calculation. The Double-K model (Jenq and Shah 1985) offers the possibility to predict the whole process of the fracture evolution and instability of the concrete material and structure, and has been proven to be effective in many cases (Zhang and Xu *et al*. 2007; Kumar and Pandey 2012; Ince2010a, 2010b; Jolivet *et al*. 2007; Kumara and Barai 2009). Xu and Reinhardt (1999a, 1999b, 1999c, 2000) proposed that the three-point bending beam test is an accurate, simple and convenient standard test to obtain Double-K fracture parameters. However, the double-K model has been rarely utilized to investigate the softening behavior of polypropylene fiber-reinforced concrete.

It is well known that with the loading increasing, a local high strain band would manifest gradually in the concrete, even in polypropylene fiber–reinforced concrete structure, which has always been considered as an inevitable precursor of brittle fracture (Rouchier *et al*. 2013). The micro-crack and damage behavior could happen in the local high strain band, while the other zone of the structure is still under elastic state (Hutchinson and Suo 1992; Beuth 1992; Zhu *et al*. 2012). The evolution of the local high strain band must be tracked in order to evaluate the fracture toughness of brittle fracture materials such as concrete and rock.

### *1.2 Objective and scope*

The objectives of this paper are to investigate the fracture behavior of polypropylene fiber reinforced concrete and to propose a proper content of such fiber in a specific concrete to guarantee great fracture toughness, as well as good strength. The digital speckle correlation method was employed to monitor the whole experiment process and to observe the initialization and evolution of local high strain band in concrete with different volumes of polypropylene fiber contents. The length values of the local high strain bands in concrete were measured and then employed to calculate the fracture toughness using the concrete fracture mechanics. This paper also provided an alternate method in evaluating the fracture behavior of fiber-reinforced concrete. The Double-K fracture theory was utilized to calculate the fracture energy of concrete, which explored the different softening behaviors of fiber-reinforced concrete with different fiber contents. In the end, an appropriate fiber content was recommended for the fiber reinforced concrete so that the concrete obtained good strength and toughness to resist fracture.

## 2. Test of three-point bending beams

### *2.1 Preparation of polypropylene fiber reinforced concrete beam*

The concrete used in this paper have different volumetric contents of polypropylene fibers, including 0%, 0.2%, 0.4%, 0.8%, 1.6%, 3.2%. The concrete beam sketch is shown in Fig. 1. The size of each beam is as follows: L = 700 mm, D = 150 mm, H = 75 mm. The size of initial notch is as follows: a = 75 mm, w = 5 mm. Wooden molds were used to make concrete beams. The FRC beams were kept in the curing room for 28 days. The following materials were used in the specimen of three-point bending FRC beam: ordinary portland cement, river sand, crushed stone with the maximum size of 10.0 mm, silica powder, water-reducing admixture and tapwater for mixing and curing. The polypropylene fibers with a length of 6.0 mm and a diameter of 0.175 mm were added to cement concrete, as shown in Fig. 2.

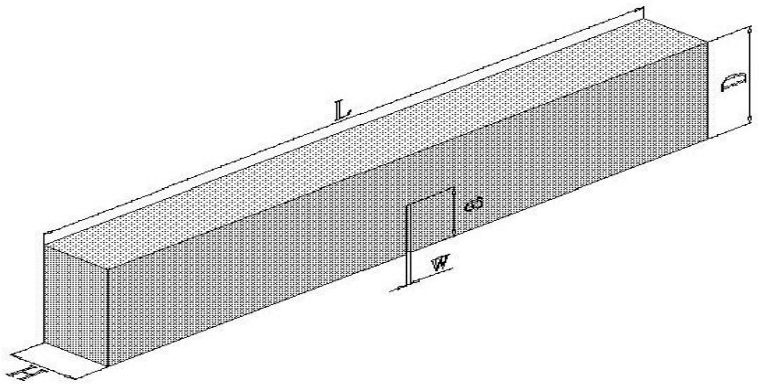


Fig. 1 The Sketch of specimens


Fig. 2 The polypropylene fiber used in the test

### 2.2 Laboratory test

According to the ASTM E399-09 (2009), the FRC beams are notched after molded and cured. Then the FRC beams are employed in the three-point bending tests in the MTS 810 (Material test system 810) produced by USA, whose maximum load is 100 kN (see Fig. 3). According to ISO 9597 (2002), the test temperature is 20°C ± 2°C. During the tests, the computer records all applied loads. According to the standard ASTM E399-09(2009), the three-point bending test mainly focuses on evaluating the mode I fracture behavior of concrete. However, the forms of the supports may have influences on the mode I fracture behavior of concrete beam. Therefore, the rolling supports used in the tests were smeared with the engine oil before each test.

In order to investigate the local deformation band of the FRC before cracking, we monitored the whole cracking process of concrete beam with the digital speckle correlation method (DSCM).

The speckle points were disposed, as shown in Fig. 4. In this test, the high brightness LED lamps were used to illuminate forward and the complementary metal-oxide semiconductor camera (short for CMOS) was used to collect data with a frequency of one fame per second, which was stored directly in the computer. The whole process of monitoring and data collection is shown in Fig. 5.

For the tests of three-point bending concrete beams with notch, the key criterion of evaluating fracture resistance is the pressure-cracking mouth opening displacement (P-CMOD) curve. In these tests, two large white speckle points at the corners of the notch were used to measure the CMOD, as shown in Fig. 6. The reason is that the areas of notched concrete beam are in the elastic state in the cracking process except for the fracture process zone. Therefore, the relative displacement between the two speckle points, where the stress levels are always very low, can generally reflect the CMOD.

Fig. 3The FRC specimen with rolling supports

Fig. 4 The speckle field made in the test

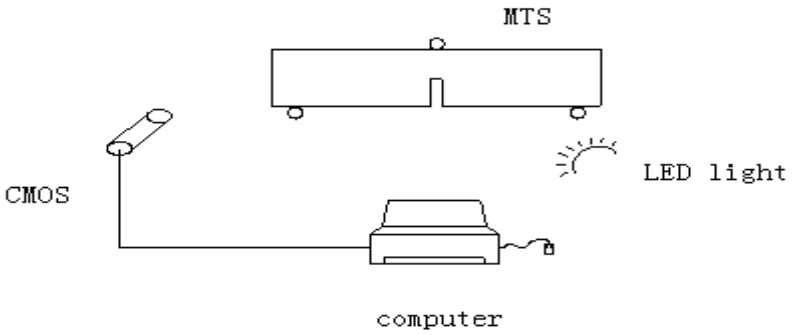


Fig. 5 The test equipment of DSCM

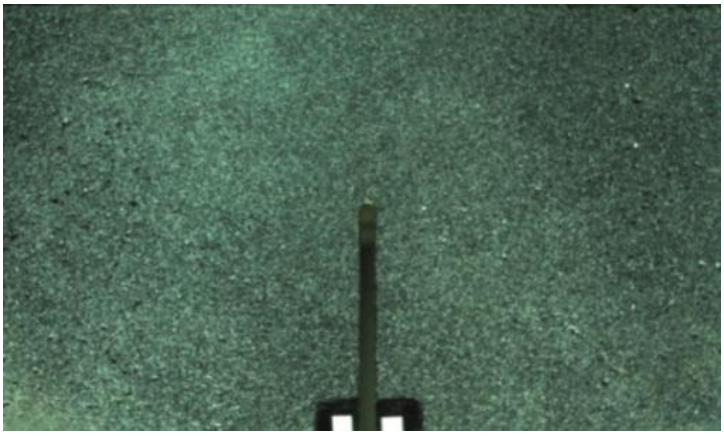

Fig. 6 CMOD data collection points

### 2.3 Results analysis

The P-CMOD curves of notched concrete beams with different volumes of fiber contents were shown in Figs. 7-8, where the loading rates were 0.1 mm/min and 0.2 mm/min, respectively. From the plain concrete test results, it can be found that the P-CMOD curves fell down immediately to nearly zero after the corresponding peak values, and the material lost its load-carrying capacity. This phenomenon reflects the quasi-brittle fracture characteristic of plain concrete material, and indicates that the loading rates have little influence on the test results. When the volumetric content of fiber reaches 0.2%, the P-CMOD curves still fell down. However, the applied loads stabilized on about 0.3 kN for a long time. This phenomenon indicates that the specimens remain about 10% of the initial load-carrying capacity, which is called as *the residual strength*. The reason why the residual strength exists in the FRC is that the fibers can prevent the concrete from rapid cracking. The loading rates have little influence on the results in these tests. When the volume of fiber contents reaches 0.4%, the P-CMOD curves are similar to those with the fiber content 0.2%, while the residual strength of the FRC increases almost 20% of the initial strength. When the volume of fiber contents reaches 1.6%, the residual strength can be 50% of the initial strength, and the influences of loading rates on the test results still are not significant. However, when the volume of fiber contents reaches 3.2%, the loading rates have significant influences on the test results. When the loading rate is 0.1mm/min, the residual strength of the FRC can reach 80% of the initial strength. On the other hand, when the loading rate reaches 0.2 mm/min, the residual strength is only approximate 60% of the initial strength. Indeed, the improvement of residual strength can reflect the increase in the fracture resistance of the FRC, and the fiber has significant influences on the toughness of concrete.

The toughening mechanism of the FRC is determined by two aspects: one is the strength of the fiber itself and the other is the bonding capacity between the fiber and the concrete. From the tests, all the fibers were not broken during the whole process of tests, which indicates that the tensile strength of fiber is much stronger than the bonding capacity. Therefore, the toughening mechanism of the FRC is mainly determined by the bonding capability between the fiber and the concrete.

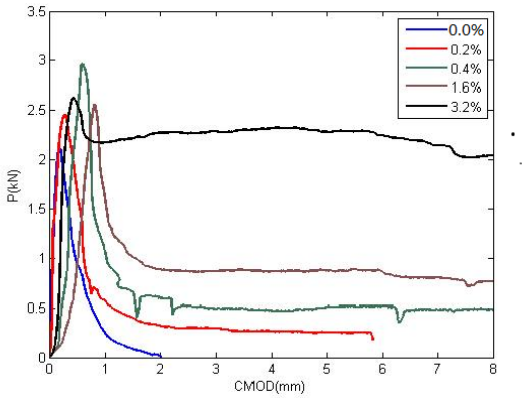


Fig. 7The P-CMOD curves with different fiber contents (loading rate 0.1 mm/min)

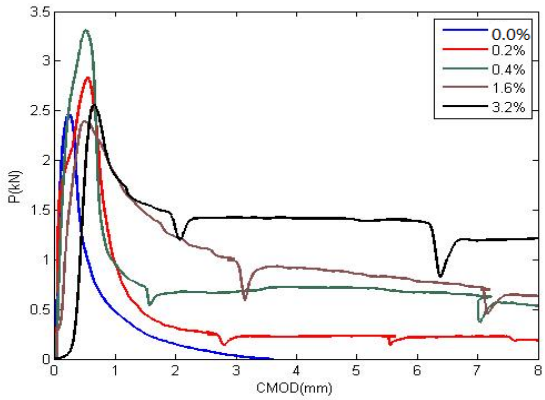


Fig. 8The P-CMOD curves with different fiber contents (loading rate 0.2 mm/min)

As a result, the phenomenon of residual strength in the P-CMOD curves can be regarded as follows: with the increase of the cracking, the adherence capability of concrete gradually decreases and the fibers become the main carriers to bear the applied loads. As the test continues, the bonding zone between the fibers and concrete is gradually destroyed, and the residual strength of the FRC is exhibited and retained. When the interfaces between the fibers and concrete are totally damaged, the fibers are extracted from the concrete. It shows that the failure of bonding zone between the fibers and concrete leads to the final damage of specimen.

## 3. Local deformation bond of the three-point bending beam

### *3.1 Displacement and strain field of the plain concrete beam*

The digital speckle pictures of the displacement field change with time. Figs. 9(a)-(d) shows the displacement changes at different time since started (625, 677, 702 and 723 seconds) for the

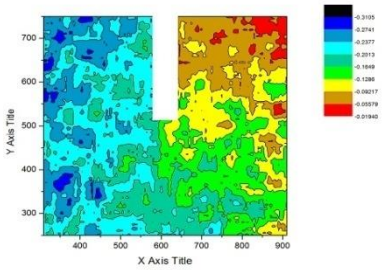


a) at 625 second

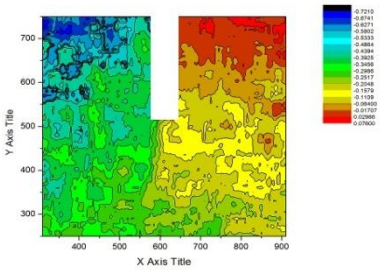


b) at 677 second

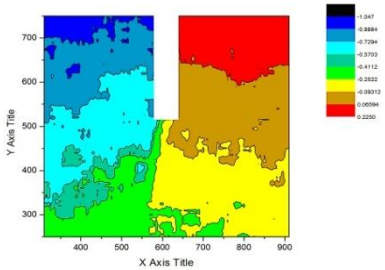


c) at 702 second

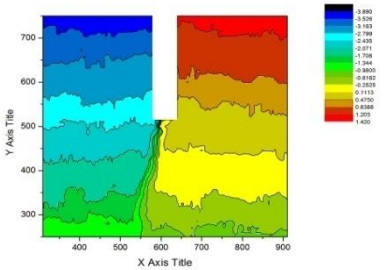


d) at 723 second

Fig. 9 The horizontal displacement fields of plain concrete at the loading rate of 0.2mm/mi**n**

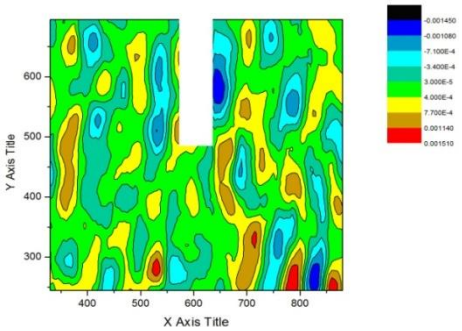


a) at 625 second

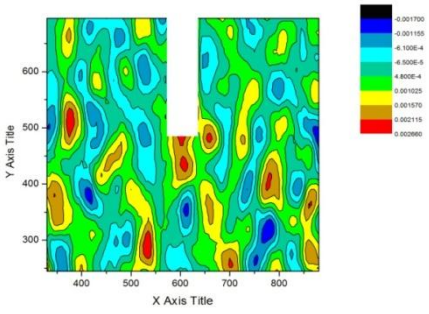


b) at 677 second

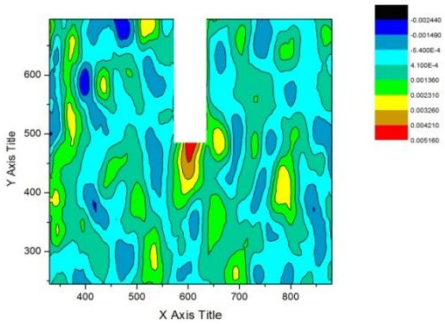


c) at 702 second

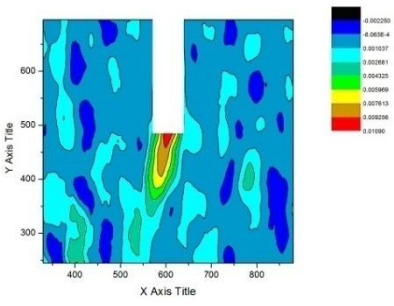


d) at 723 second

Fig. 10 The horizontal strain fields of plain concrete at the loading rate of 0.2mm/mi**n**

ordinary cement concrete. It can be seen that with the increasing of applied load, the initial uniform distribution gradually changes to a gradient distribution for the horizontal displacement of the concrete specimen.

The digital speckle pictures of the strain field evolution with time are shown in Fig. 10(a)-(d), where the horizontal strain distributions at different time points (625, 677, 702 and 723 seconds) are respectively shown in Fig. 10(a)-(d). With the increasing of the applied load, the horizontal strain of the local deformation band changes obviously.

Under the stable loading condition, the strains in the local deformation band are much higher than those in the other zones. When the applied load reaches the maximum value, the maximum horizontal strain is approximately 0.01in the center zone while the strains are only 0.001~0.002 in other zones. It indicates that the strains in the local deformation band change greatly and are almost 10 times higher than those in the other zones.

### *3.2 Strain field of FRC beams with different volumetric fiber contents*

When the maximum loads are applied on the concrete beams, the horizontal strain fields of the FRC with different fiber contents and loading rates are shown in Figs. 11 (a)-(j). The results show that the prominent high strain zone appears in the middle of the beam and distributes as a local

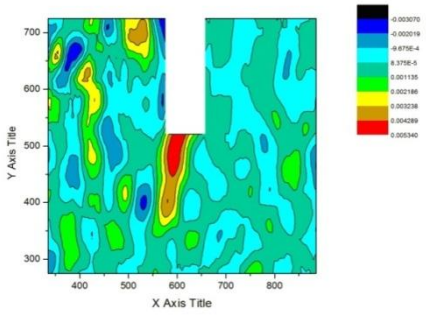


a) plain concrete at the 0.1mm/min loading rate

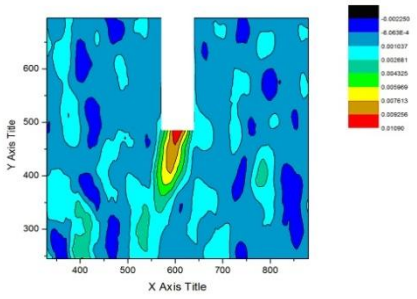


b) plain concrete at the 0.2mm/min loading rate

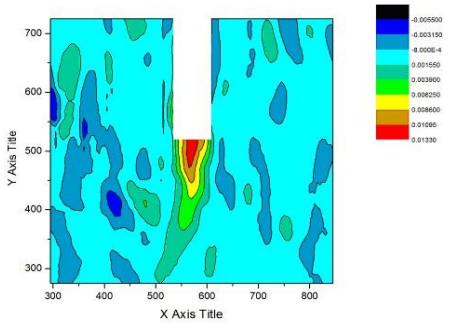


c) 0.2% fiber at the 0.1mm/min loading rate

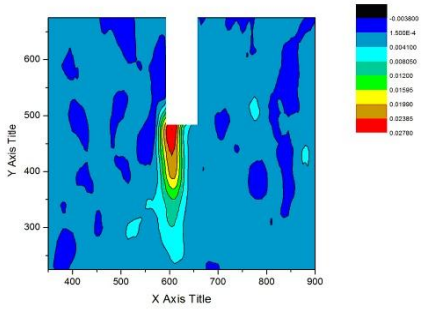


d) 0.2% fiber at the 0.2mm/min loading rate

Fig. 11 The horizontal strain fields of FRC with low fiber contents and loading rates under the maximum applied load

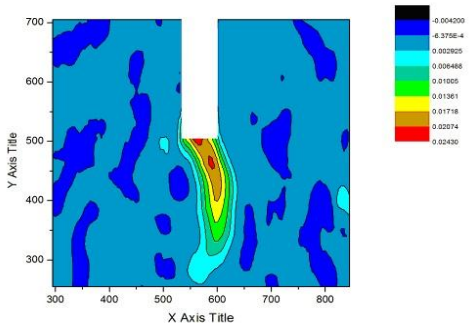


e) 0.4% fiber at the 0.1 mm/min loading rate

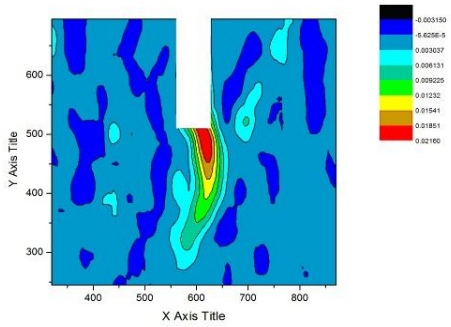


f) 0.4% fiber at the 0.2 mm/min loading rate

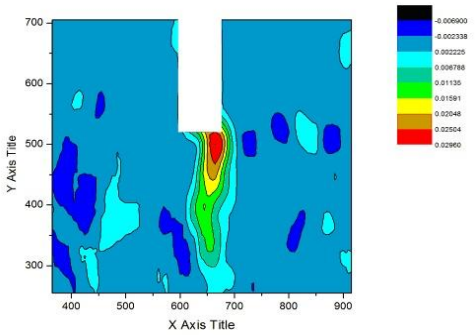


g) 1.6% fiber at the 0.1 mm/min loading rate

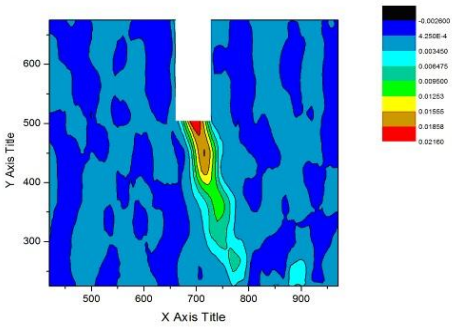


h) 1.6% fiber at the 0.2 mm/min loading rate

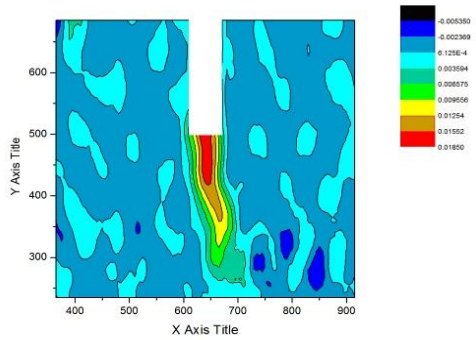


i) 3.2% fiber at the 0.1 mm/min loading rate

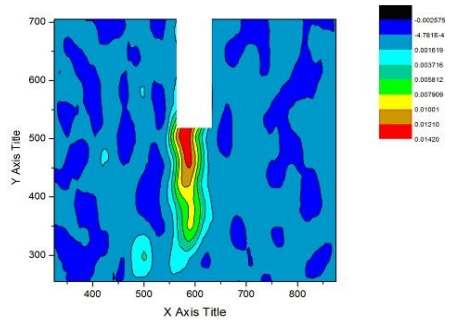


j) 3.2% fiber at the 0.2 mm/min loading rate

Fig. 11 Continued

deformation band. Meanwhile, the horizontal strains in this zone are much higher than those in the other zones.

Take the tests at the loading rate of 0.1 mm/min for example, from the results of the horizontal strain fields of the FRC with different volumes of fiber contents, it is found that with the increasing of the fiber contents(ranging from 0% to 1.6%), the maximum strains corresponding to the peak loads gradually increase. When the volume of fiber contents is 1.6%, the maximum horizontal strains are bigger than others. However, when the fiber content exceeds 1.6%, the maximum strain decreases, and is lower than that of the FRC with fiber content 0.4%.

It indicates that 3-dimensional spacious network structures in the concrete are formed easily

after adding the fibers to concrete, when the volume of the fiber contents is appropriate. 3-dimensional spacious network structures can resist the growth of micro-cracks in concrete, and improve the capability of concrete material to bear the higher deformation.

If the fiber content is higher than 1.6%, the excessive fibers will form the structures such as sieves, which can lead to the segregation between coarse aggregates and fine aggregates, which will cause the decline of the strength of concrete material.

## 4. Analysis on fracture behavior of the FRC beams based on the double-*K* theory with softening behavior

Based on the previous digital speckle test results, it can be found that an obvious local deformation band developed during the loading process. The initial local deformation band has manifested when the loading is around the peak value referred to P-CMOD curves (Figs.7 and 8), and the length of local deformation band will reach the maximal value before ultimate unstable fracture.

There are varieties of fracture models on the three-point bending test of notched concrete beam in literature. The Double-*K* model calculation method (Tada *et al*. 2000) can predict the cracking initiation and instability of concrete structures very well and has been widely used in engineering fracture analysis. However, the Double-K model has defects in predicting the FRC fracture behavior, as it does not include the softening behavior and fracture toughness since different fiber volume contents cannot be accurately described. Therefore, it is necessary to develop a modified Double-K model considering the softening behavior.

According to the Double-K fracture model, the variable *CMOD* is calculated as follows:

$$CMOD = \frac{24P}{EB} V F_1(V) \tag{1}$$

where $E$ is the elastic modulus of material, $P$ is the load, $B$ is the thickness of beam and the expression of $F_1(V)$ is as follows:

$$F_1(V) = 0.76 - 2.28V + 3.87V^2 - 2.04V^3 + \frac{0.66}{(1-V)^2} \tag{2}$$

where $V = a/D$, $a$ is the length of initial notch, and $D$is the height of beam.

Jenq and Shah (1985) simplified the expression $F_1(V)$ to find an approximate formula for calculating the crack length of the three-point bending beam.

$$CMOD = \frac{P}{BE}[3.70 + 32.60\tan^2(\frac{\pi}{2}V)] \tag{3}$$

Then

$$V = -\frac{2}{\pi}\arctan\sqrt{\frac{B \cdot E \cdot CMOD}{32.6 \cdot P} - 0.1135} \tag{4}$$

It was concluded that when $V$ is between 0.2 and 0.75, the error is under 2.0% and when $V$ is 0.8, the error cannot exceed 3.5%. So the equivalent crack length at any time is:

$$a = -\frac{2}{\pi} D \cdot \arctan\sqrt{\frac{B \cdot E \cdot CMOD}{32.6 \cdot P} - 0.1135} \tag{5}$$

Since there is a relationship between the stress intensity factor and the adhesion force in the adhesion zone, the stress intensity factor at any time can be described as follows (as shown in Fig. 12):

$$K_{\mathrm{I}}^{\mathrm{C}} = -\int_{a_0}^{a} \frac{2\sigma(x/a)}{\sqrt{\pi a}} F(\frac{x}{a}, \frac{a}{D}) dx \qquad (a \le a_c) \tag{6}$$

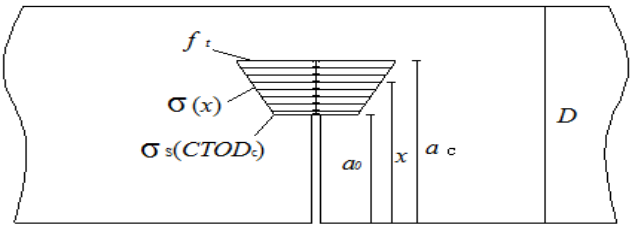


Fig. 12 Cohesive force on the fictitious crack zone at the critical situation

If we use $K_{\mathrm{I}}^{\mathrm{C}} / f_t \sqrt{D}$ to dimensionalize the stress intensity factor, then we can use $V = a/D$, $V_0 = a_0/D$ and $U = x/a$ to dimensionalize Eq.(6) as follows:

$$K_I^C / f_t \sqrt{D} = -2\int_{V_0/V}^{1} \sqrt{\frac{V}{\pi}} \frac{\sigma(U)}{f_t} F(U,V) dU \tag{7}$$

where

$$F(U,V) = \frac{3.52(1-U)}{(1-V)^{3/2}} - \frac{4.35-5.28U}{(1-V)^{1/2}} + \{\frac{1.30-0.30U^{3/2}}{[1-U^2]^{1/2}} + 0.83 - 1.76\} \times [1-(1-U)V] \tag{8}$$

Xu and Reinhard (2000) simplified the above equation as follows:

$$F(U,V) = AU + B + \frac{1}{\sqrt{1-u^2}} \tag{9}$$

where

$$A = -\frac{2.23V^2 + 1.16V + 0.17}{(1-V)^{3/2}} \ , \ B = \frac{1.65V^2 + 1.67V + 0.24}{(1-V)^{3/2}} \tag{10}$$

On the other hand, the distribution of adherence load $\sigma(x)$ in the virtual crack zone can be expressed as follows:

$$\sigma(x) = \sigma_s(CTOD_c) + \frac{x-a_0}{a_c-a_0}[f_t - \sigma_s(CTOD_c)] \quad (a_0 \le x \le a_c) \tag{11}$$

where $\sigma_s(CTOD_c)$ stands for the stress when the $CMOD$ reaches the critical value $\sigma_s(CTOD_c)$, and $CMOD$ can be calculated with the following empirical equation:

$$CTOD = CMOD\{(1-\frac{a_0}{a})^2 + (1.081 - 1.149\frac{a}{D})[\frac{a_0}{a} - (\frac{a_0}{a})^2]\}^{1/2} \tag{12}$$

So the Eq.(11) can be simplified as follows:

$$\sigma(x) = Cx + E \tag{13}$$

where $C = \frac{f_t - \sigma_s}{V - V_0}$, $E = \frac{V\sigma_s - V_0 f_t}{V - V_0}$, in which $\sigma_s$ can be calculated by the softening curve.

Substituting Eqs. (7) - (13) into Eq. (6), the critical adherence fracture toughness can be conducted as follows:

$$K_{\mathrm{IC}}^{\mathrm{C}} = 2\sqrt{\frac{a_c}{\pi}}\left[\frac{A\cdot D}{3}U^3 + \frac{A\cdot E + B\cdot D}{2}U^2 + B\cdot E\cdot U - D\sqrt{1-U^2} + E\cdot \arcsin(U)\right]_{V/V_{0c}}^{1} \tag{14}$$

For the quasi-brittle material, the unstable toughness and the initial toughness can be related with the bonding toughness.

$$K_{\mathrm{IC}}^{\mathrm{un}} = K_{\mathrm{IC}}^{\mathrm{ini}} + K_{\mathrm{IC}}^{\mathrm{C}} \tag{15}$$

Through the above equation, the unstable toughness can be calculated with the initial toughness and the bonding toughness. Besides, we can calculate the initial toughness of three-point bending beam with the equation (Tada *et al*. 2000) as follow:

$$K_{\mathrm{IC}}^{\mathrm{ini}} = \frac{3P_{\mathrm{ini}}S}{2D^2B}\sqrt{a_0}F_1\left(\frac{a_0}{D}\right) \tag{16}$$

$$F_1\left(\frac{a_0}{D}\right) = \frac{1.99 - \left(\frac{a_0}{D}\right)\left(1-\frac{a_0}{D}\right)\left[2.15 - 3.93\frac{a_0}{D} + 2.7\left(\frac{a_0}{D}\right)^2\right]}{\left(1+2\frac{a_0}{D}\right)\left(1-\frac{a_0}{D}\right)^{\frac{3}{2}}} \tag{17}$$

where $P_{\mathrm{ini}}$ is the load responding to the time when the concrete begins to crack, $a_0$ is the length of initial notch, and B, D, S are the width, height and span of the specimen, respectively.

For the ordinary plain concrete, the calculation of stress intensity factor at the time of instability is similar to Eqs. (4)-(16)

$$K_{\mathrm{IC}}^{\mathrm{un}} = \frac{3P_{\max}S}{2D^2B}\sqrt{a_c}F_1\left(\frac{a_c}{D}\right) \tag{18}$$

where $P_{\max}$ is the maximum value in the P-CMOD curve and $a_c$ is the critical crack length when the crack begins to unstably develop (as shown in Fig. 12), and this value as the high strain band length can be measure using digital speckle method.

It has been shown above that the structure fracture behavior with adherence force, which occurs during the crack evolution in three-point bending FRC beam, can be accurately simulated. Based on the modified Double-K fracture model, the Double-Kcritical values of FRC beam under three-point bending test can be calculated.

The calculated fracture parameters are listed in Table 1. It can be seen that when the volume of fiber content reaches 3.2%, the fracture energy of the FRC can reach 8342 N/m, which is 47 times of the plain concrete (177 N/m). The fibers can obviously improve the fracture resistance of concrete material. The unstable fracture toughness of the FRC was enhanced from 2.22MPa·m$^{1/2}$ to 96.38MPa·m$^{1/2}$, which is larger than common metal materials. Meanwhile, the initial fracture toughness of the FRC keeps in the low level even with different fiber contents. A reasonable explanation is as follows: with the increasing of volume of fiber content, intense and prominent

Table 1 The calculated fracture parameters with different fiber contents

| Fiber Contents | Loading rates (mm/min) | Fracture energy $G_f$ (N/m) | $K_{IC}^{ini}$ (MPa·m$^{1/2}$) | $K_{IC}^{un}$ (MPa·m$^{1/2}$) |
|---|---|---|---|---|
| 0.0% | 0.1 | 177 | 0.67 | 2.22 |
| | 0.2 | 244 | 0.64 | 2.07 |
| 0.2% | 0.1 | 421 | 0.69 | 2.41 |
| | 0.2 | 527 | 0.72 | 3.16 |
| 0.4% | 0.1 | 858 | 0.73 | 10.23 |
| | 0.2 | 1148 | 0.67 | 8.19 |
| 1.6% | 0.1 | 1627 | 0.79 | 29.28 |
| | 0.2 | 1771 | 0.52 | 16.85 |
| 3.2% | 0.1 | 8342 | 0.66 | 96.38 |
| | 0.2 | 5004 | 0.40 | 60.95 |

ductile behaviors appear in the P-CMOD curves as metal material, which was just observed in the previous experiments. The volume of fiber content in the concrete is very significant for enhancing the fracture resistance of the FRC.

It should be mentioned that concrete with 3.2% fiber content has the largest unstable fracture toughness while has lower initial fracture toughness than concrete with 1.6% fiber. In the field, the strength, which is proportional to the initial fracture toughness, has affinity with the service life of the pavement. Therefore, the concrete with 1.6% fiber is the most suitable for pavement construction.

## 5. Investigation on the fracture behavior of PFRC beam with initial notch using Xfem coupling with VCCT criterion

After the initial fracture energy and unsteady fracture energy in the PFRC Beam with initial notch were calculated from the Double-K fracture model, the fracture behavior of this kind of beam was simulated with the extended finite element method (short for Xfem) and using virtual crack closure technical (short for VCCT) in the following part.

The extended finite element method was first introduced by Belytschko and Black (1999). Unger *et al*. (2007) and Chahine *et al*. (2008) introduced Xfem into researching fracture behaviors of plain concrete materials. It is an extension of the conventional finite element method based on the concept of partition of unity, which allows local enrichment functions to be easily incorporated into a finite element approximation. The presence of discontinuities is ensured by the special enriched functions in conjunction with additional degrees of freedom. Crack modeling based on Xfem allows for simulation of both stationary and moving cracks. Evaluation of crack contour integrals with Xfem is available for three dimensional analyses. Simulation of propagating cracks with Xfem does not require initial crack and crack path definitions to conform to the structural mesh. The crack path is solution dependent, i.e., it is obtained as part of the solution. Cracks are allowed to propagate through elements allowing for modeling of the fracture of the bulk material.

For the purpose of fracture analysis, the enrichment functions typically consist of the near-tip asymptotic functions that captures the singularity around the crack tip and a discontinuous function that represents the jump in displacement across the crack surfaces. The approximation for a displacement vector function with the partition of unity enrichment (Kesler *et al*. 1972) is described by the Eq. (19).

$$\mathbf{u} = \sum_{I=1}^{N} N_I(x)[\mathbf{u}_I + H(x)\mathbf{a}_I + \sum_{\alpha=1}^{4} F_\alpha(x)\mathbf{b}_I^\alpha] \tag{19}$$

where $N_I(x)$ are the usual nodal shape functions; $\mathbf{u}_I$ is the usual nodal displacement vector associated with the continuous part of the finite element solution; the second term is the product of the nodal enriched degree of freedom vector, $\mathbf{a}_I$ and the associated discontinuous jump function $H(x)$ across the crack surfaces; and the third term is the product of the nodal enriched degree of freedom vector, $\mathbf{b}_I^\alpha$, and the associated elastic asymptotic crack-tip functions, $F_\alpha(x)$. The first term on the right-hand side is applicable to all the nodes in the model; the second term is valid for nodes whose shape function support is cut by the crack interior; and the third term is used only for nodes whose shape function support is cut by the crack tip. *H*(*x*) can be written as Eq. (20).

$$H(x) = \begin{cases} 1 & if\ (x - x^*) \cdot n \geq 0 \\ -1 & otherwise \end{cases} \tag{20}$$

where *x* is a sample (Gauss) point, $x^*$ is the point on the crack closest to *x*, and *n* is the unit outward normal to the crack at $x^*$ (Fig.13).

The asymptotic crack tip functions in an isotropic elastic material, $F_\alpha(x)$, which are given by Eq. (21).

$$F_\alpha(x) = [\sqrt{r}\sin\frac{\theta}{2}, \sqrt{r}\cos\frac{\theta}{2}, \sqrt{r}\sin\theta\cdot\sin\frac{\theta}{2}, \sqrt{r}\sin\theta\cdot\cos\frac{\theta}{2}] \tag{21}$$

where ($r$, $\theta$)a polar coordinate system with its origin at the crack is tip and $\theta$ =0 is tangent to the cracking tip.

Crack initiation refers to the beginning of degradation of the cohesive response at an enriched element. The process of degradation begins when the stresses or the strains satisfy specified crack initiation criteria. We use the initial fracture energy of double-K model to transfer to a stress value as the crack initiation criteria.

The VCCT was first introduced by Rybicki and Kanninen (1977). Initially it was called Modified Crack-Closure Integral (MCCI), subsequently renamed to Virtual Crack Closure Technique. Raju (1987) wanted to explain legitimately VCCT with mathematics and provided the computational formula according to higher order element and singular element. The VCCT is based on the assumption that the strain energy released when a crack is extended in a certain amount is the same as the energy required to close the crack in the same amount. Assuming that the crack closure is governed by linear elastic behavior, the energy to close the crack (and thus, the energy to open the crack) is calculated from the Eq. (22).

$$\int_0^{\Delta a} \sigma_{yy}^{(1)}(x)\Delta v^2(x)dx = F_{y1}^{(1)} v_{1,1'}^{(2)} \tag{22}$$

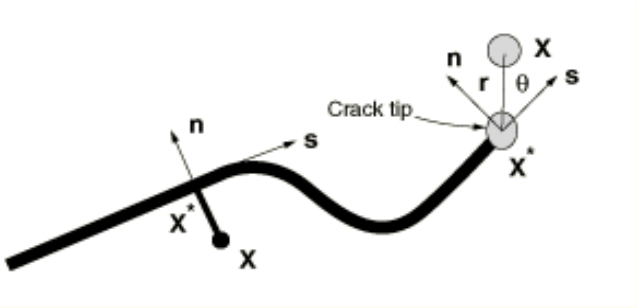


Fig. 13 Illustration of normal and tangential coordinates for a smooth crack

Table 2 the parameters of the VCCT model

| Young's Modulus (MPa) | Poisson's Ratio | Density ($Kg/m^3$) | MAXPS Damage (MPa) | $G_I$ (N/mm) | $G_{II}$ (N/mm) | $G_{III}$ (N/mm) |
|---|---|---|---|---|---|---|
| 30000 | 0.25 | 2500 | 1 | 0.1 | 0.02 | 0.02 |

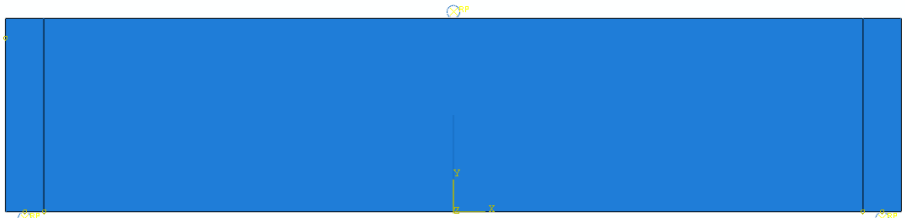

a) without mesh

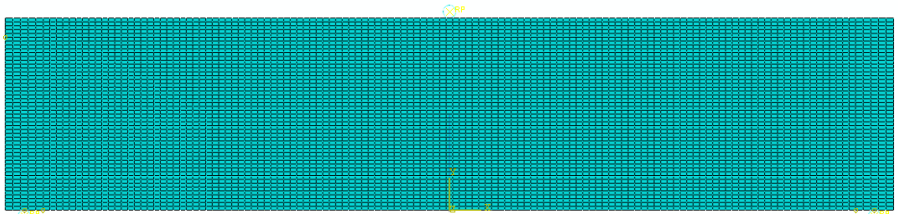

b) with mesh

Fig. 14the FEM model of three-point bending beam with initial notch

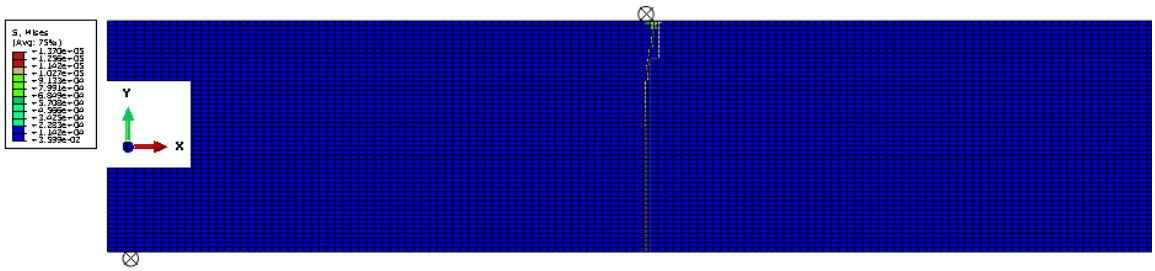


Fig. 15 The ultimate fracture style of the three-point bending beam numerical test

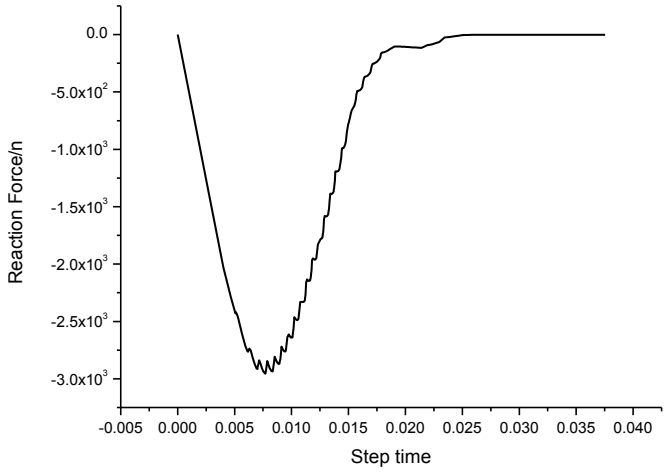


Fig. 16 The reaction force curve of the indenter in numerical test

where, $\Delta a$ is the crack extended length.

Based on the VCCT crack evolution criterion, the unsteady fracture energy of double-K model replace the strain energy released during the fracture evaluation procedure. The parameters, which have reflected the fracture toughness with 0.2% volume contents, used in the numerical test have been listed in Table 2.

We used the finite element software Abaqus to simulate fracture behavior of the PFRC beam. The finite element model was shown in Fig. 14(a)-(b). The three-point bending beam was meshed with 67504-node bilinear plane stress quadrilateral elements. The simulated ultimate fracture type was shown in Fig.15. The fracture behavior has manifested mixture crack type, and the reaction force of the indenter was shown in Fig. 16. The numerical simulation results provided almost the same values on the peak value and soften behavior with the experiment.

## 6. Conclusions

This paper studied the fracture tests of three-point bending notched concrete beam with different fiber contents and obtained the P-CMOD curves of the beam. To evaluate the fracture toughness of concrete, the DSCM techniquewas utilized to observe the local deformation band in the crack evolution of concrete beam. A modified Double-K fracture model considering the softening behavior was developed to describe the fracture behavior of FRC beam. Through the P-CMOD curves and the modified Double-K model with the softening behavior, the initial and unstable stress intensity factors and respective fracture toughness were obtained. Several conclusions can be drawn as follows:

- The modified Double-K model can explain the influence of softening behaviors of the FRC and provide a more reasonable standard to differentiate the fracture toughness of concretes with different fiber volume contents.

- With the increase of the fiber content, there is a residual strength after the peak value in the P-CMODcurve and the residual strength ascends with the increase of the fiber content. When the fiber content reaches 3.2%, the residual strength will be 60%~80% of the initial strength.
- There is a local deformation band in the crack evolution of the fiber concrete beam, and the horizontal tension strain is approximately 10 times of that outside the local deformation and.
- The increase of the fiber content can improve the unstable fracture critical toughness of concrete distinctly and it has little influence on the initial fracture critical toughness.
- The modified Double-K fracture model developed in this paper can effectively evaluate the fracture behavior of fiber-reinforced concrete.
- In order to balance the strength and resistant fracture toughness, concrete with 1.6% fiber to be applied in pavement construction is recommended.
- The Xfem coupling with the VCCT criterion was utilized to evaluate the fracture behavior of PFRC beam, where the parameters of VCCT were transferred from the Double-K model. Furthermore the numerical result has manifest consistency with the experiment results.

## Acknowledgments

This research was supported by the China Ministry of Communications (Project No. 19672016). The contents of this paper reflect the views of the authors, who are solely responsible for the facts and the accuracy of the data presented herein, and do not necessarily reflect the official views or policies of the China Ministry of Communications, nor do the contents constitute a standard, specification, or regulation.

## References

Banthia, N. and Nandakumar, N. (2003), "Crack growth resistance of hybrid fiber reinforced cement composites", *Cement Concrete Compos*., **25**(1), 3-9.

Belytschko, T. and Black, T. (1999), "Elastic crack growth in finite elements with minimal remeshing", *Int. J. Numer. Meth. Eng*., **45**(5), 601-620.

Beuth, J.J. (1992), "Cracking of thin bonded films in residual tension", *Int. J. Solids Struct.*, **29**(13), 1657-1675.

Chahine, E., Laborde, P. and Renard, Y. (2008), "Crack tip enrichment in the XFEM using a cutoff function", *Int. J. Numer. Meth. Eng*., **75**(6), 629-646.

Dugdale, D. (1960), "Yielding of steel sheets containing slits", *J. Mech. Phys. Solids*, **8**(2), 100-104.

ASTM E399-08 A (2009), *Standard Test Method for Linear-Elastic Plane-Strain Fracture Toughness KIC of Metallic Materials*, West Conshohocken, PA, 19428-2959 USA.

EN T. 196-3 (2002), Methods of testing cement-part 3: determination of setting time and soundness. Turkish Standards Institution, Turkey.

Hillerborg, A., Modéer, M. and Petersson, P.E. (1976), "Analysis of crack formation and crack growth in concrete by means of fracture mechanics and finite elements", *Cement Concrete Res*., **6**(6), 773-781.

Hutchinson, J. and Suo, Z. (1991), "Mixed mode cracking in layered materials", *Adv. Appl. Mech*., **29**(63), 163-191.

Ince, R. (2010), "Artificial neural network-based analysis of effective crack model in concrete fracture", *Fatigue. Fract. Eng. Mater. Struct*., **33**(9), 595-606.

Ince, R. (2010), "Determination of concrete fracture parameters based on two-parameter and size effect models using split-tension cubes", *Eng. Fract. Mech*., **77**(12), 2233-2250.

Jenq, Y. and Shah, S.P. (1985), "Two parameter fracture model for concrete", *J. Eng. Mech. ASCE*, **111**(10), 1227-1241.

Jolivet, D., Bonen, D.M. and Shah, S.P. (2007), "The corrosion resistance of coated steel dowels determined by impedance spectroscopy", *Cement Concrete Res*, **37**(7), 1134-1143.

Kaplan, M. (1961), "Crack propagation and the fracture of concrete", *ACI Journal proceedings: ACI*, December.

Katz, A. and Bentur, A. (1994), "Mechanical properties and pore structure of carbon fiber reinforced cementitious composites", *Cement Concrete Res*., **24**(2), 214-220.

Kesler, C.E., Naus, D.J. and Lott, J.L. (1972), "Fracture mechanics-its applicability to concrete", *Proceedings of the Society of Materials Science Conference on the Mechanical Behavior of Materials*, 113-124, May.

Kumar, S. and Barai, S.V. (2009). "Determining double-K fracture parameters of concrete for compact tension and wedge splitting tests using weight function", *Eng. Fract. Mech*., **76**(7), 935-948.

Kumar, S. and Pandey, S.R. (2012), "Determination of double-K fracture parameters of concrete using split-tension cube test", *Comput. Concr*., **9**(2), 81-97.

Ngo, D. and Scordelis, A. (1967), "Finite element analysis of reinforced concrete beams", *ACI Journal Proceedings: ACI*, March.

Oh, B. and BAZANT, Z. (1983), "Crack band theory for fracture of concrete", *Mater. Struct*., January-February, 155-177.

Raju, I. (1987), "Calculation of strain-energy release rates with higher order and singular finite elements", *Eng. Fract. Mech*., **28**(3), 251-274.

Ramli, M., Kwan, W.H. and Abas, N.F. (2013), "Strength and durability of coconut-fiber-reinforced concrete in aggressive environments", *Constr . Build. Mater*., **38**, 554-566.

Rashid, Y. (1968), "Ultimate strength analysis of prestressed concrete pressure vessels", *Nucl. Eng. Des*., **7**(4), 334-344.

Rouchier, S., Foray, G., Godin, N., Woloszyn, M. and Roux, J.J. (2013), "Damage monitoring in fibre reinforced mortar by combined digital image correlation and acoustic emission", *Constr. Build. Mater*., **38**, 371-380.

Rybicki, E.F. and Kanninen, M. (1977), "A finite element calculation of stress intensity factors by a modified crack closure integral", *Eng. Fract. Mech*., **9**(4), 931-938.

Tada, H., Paris, P.C. and Irwin, G.R. (2000), *The stress analysis of cracks handbook*, ASME Press, New York, U.S.A.

Tavakoli, M. (1994), "Tensile and compressive strengths of polypropylene fiber reinforced concrete", *ACI Spec. Publication*, **142**, 61-72.

Toutanji, H.A. (1999), "Properties of polypropylene fiber reinforced silica fume expansive-cement concrete", *Constr. Build. Mater*., **13**(4), 171-177.

Unger, J.F., Eckardt, S. and Könke, C. (2007). "Modelling of cohesive crack growth in concrete structures with the extended finite element method", *Comput. Meth. Appl. Mech. Eng*., **196**(41-44), 4087-4100.

Xu, S. and Reinhardt, H.W. (1999a), "Determination of double-K criterion for crack propagation in quasi-brittle fracture, Part I: Experimental investigation of crack propagation", *Int. J. Fract*., **98**(2), 111-149.

Xu, S. and Reinhardt, H.W. (1999b), "Determination of double-*K* criterion for crack propagation in quasi-brittle fracture, Part II: Analytical evaluating and practical measuring methods for three-point bending notched beams", *Int. J. Fract*., **98**(2), 151-177.

Xu, S. and Reinhardt, H.W. (1999c), "Determination of double-K criterion for crack propagation in quasi-brittle fracture, Part III: Compact tension specimens and wedge splitting specimens", *Int. J. Fract*., **98**(2), 179-193.

Xu, S. and Reinhardt, H.W. (2000), "A simplified method for determining double-K fracture parameters for three-point bending tests", *Int. J. Fract*, **104**(2),181-209.

Zhang, X., Xu, S. and Zheng, S. (2007), "Experimental measurement of double-K fracture parameters of concrete with small-size aggregates", *Front. Architect. Civil Eng. China*, **1**(4), 448-457.

Zhu, W., Ling, L., Tang, C., Kang, Y. and Xie, L. (2012), "The 3D-numerical simulation on failure process of concrete-filled tubular (CFT) stub columns under uniaxial compression", *Comput. Concr.*, **9**(4), 257-273.

*CC*